Extended abstract: Remaining Cycle Estimation based on a Maintenance Cycle Model

Kirin Inoue[1], Koji Wakimoto[2], Kosei Ozeki[3], Toshiyuki Kuriyama[4] and Takahiko Masuzaki[5]

[1,2,3,4,5] *Mitsubishi Electric Corporation, Kamakura, Kanagawa, 2478501, Japan*

Inoue.Kirin@ab.MitsubishiElectric.co.jp
Wakimoto.Koji@df.MitsubishiElectric.co.jp
Ozeki.Kosei@aj.MitsubishiElectric.co.jp
Kuriyama.Toshiyuki@dx.MitsubishiElectric.co.jp
Masuzaki.Takahiko@dc.MitsubishiElectric.co.jp

1. Introduction

This paper presents a remaining cycle estimation method for aircraft engines, developed during our participation in the PHM 2025 Data Challenge Competition.

The features of our method are as follows:

(1) Physics-informed Feature Exploration: Through exploratory data analysis utilizing physical insights in the field of aircraft, we found good features that reflect performance degradation.

(2) Maintenance Cycle Model: We developed a model that describes cycles of performance degradation and recovery by a weighted composite of health value for each maintenance type. The model fits well with our designated features that reflect the engine performance degradation.

(3) Estimation Optimization: Taking the scoring rules into account, we optimized the estimated results by assuming probability distribution of the true values. The optimization enabled precise and stable estimation.

2. Feature Exploration

In this section, we describe the feature design aimed at capturing the target maintenance cycles, namely cycles to HPT, HPC, and WW. The available dataset contains eight snapshots recorded at different times in each aircraft operation cycle. Among these, we focus on Snapshot 4, which corresponds to take-off conditions where the engine experiences the maximum load. Based on this dataset, the following two features were defined.

(1) Isentropic Efficiency

$$y_e = \frac{T_{25}\left[\left(\frac{P_{s3}}{P_{25}}\right)^{\frac{\gamma-1}{\gamma}} - 1\right]}{T_3 - T_{25}}$$

The feature y_e represents the isentropic efficiency, where T_{25} denotes the inlet temperature of the HPC, T_3 the outlet temperature of the HPC, P_{25} the inlet pressure of the HPC, P_{s3} the outlet pressure of the HPC, and γ the specific heat ratio, assumed to be 1.4 in this study.

(2) Increment Rate from T_3 to T_{45}

$$y_t = \frac{T_{45} - T_3}{T_3}$$

The feature y_t denotes the increment rate from T_3 to T_{45}. Here, T_3 corresponds to the outlet temperature of the HPC (and inlet temperature of the HPT), and T_{45} indicates the outlet temperature of the HPT.

Correlation analysis of these features revealed that the isentropic efficiency and the increment rate from T_3 to T_{45} exhibited strong correlations with the HPC and HPT, respectively (Table 1 and Figure 1).

This result confirms that the designed features effectively capture the main target indicators. In contrast, the correlation with WW was relatively low, indicating that linear relationships alone are insufficient for explanation. However, as discussed in Chapter 5, time-series analysis of the increment rate from T_3 to T_{45} incorporating simulation data revealed repeated spikes with the same periodicity as WW, suggesting the presence of underlying periodic dependencies.

Table 1. Correlation coefficients between designed features and engine performance indicators (HPT, HPC, WW) under ESN101–Snapshot 4 condition.

	HPC	HPT	WW
Isentropic Efficiency	0.78	0.18	0.18
Increment Rate from T_3toT_{45}	-0.55	-0.94	-0.08

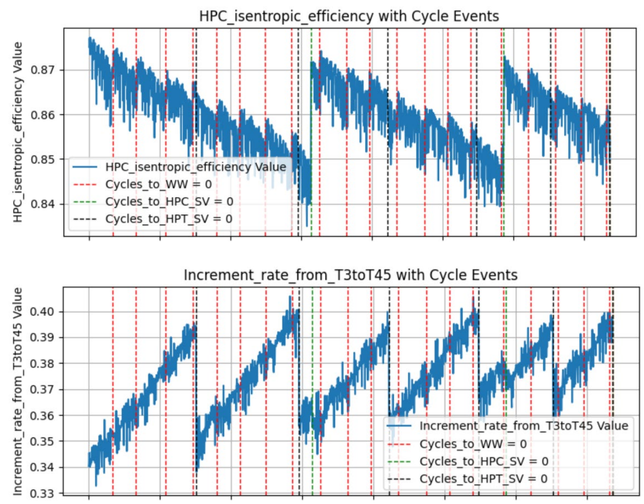

Figure 1. Time-series variations of designed features and maintenance events under ESN101–Snapshot 4 condition.

In summary, isentropic efficiency and the increment rate from T_3 to T_{45} are expected to directly contribute to the prediction of HPC and HPT. For the prediction of WW, incorporating simulation data for the increment rate from increment rate from T_3 to T_{45} suggests that, although correlation coefficients alone may not be sufficient for evaluation, this feature could demonstrate usefulness in models that account for periodic characteristics. Since the test dataset does not contain T_5 and P_{25}, we estimated them using LightGBM. In the subsequent chapters, these designed features will be utilized to explore inference approaches.

3. MAINTENANCE CYCLE MODEL

The maintenance cycle model is introduced to describe cycles of performance degradation and recovery. It is meant to be applied to situations where there are several types of maintenance conducted following their own maintenance cycles.

We assumed that each engine has a health value for each type of maintenance. As shown in Figure 2, the health values gradually decrease over cycles, and each value recovers to the original after its corresponding type of maintenance.

We assumed that observations can be estimated by a weighted composite of health values. The bottom plot in Figure 2 shows an example of the estimated observations, which is composed of 0.8 and 0.2 of health values from Maintenance A and Maintenance B, respectively.

The idea is expressed in the following equation:

$$f_i(x_i) = \sum_j a_{ij} x_j + c_i \quad (1)$$

where f_i $(i = 1 \dots n)$ are functions to estimate observation i, x_j $(j = 1 \dots m)$ are remaining cycles for maintenance j, and a_{ij} and c_i $(i = 1 \dots n, j = 1 \dots m)$ are coefficients.

The equation (1) can be rewritten as:

$$F(X) = AX + C \quad (2)$$

where $F = (f_1, \dots, f_n)$, $X = (x_1, \dots, x_m)$, $C = (c_1, \dots, c_n)$, $A = ((a_{11}, \dots, a_{1m}), \dots, (a_{n1}, \dots, a_{nm}))$.

Once we find observations $Y = (y_1, \dots, y_n)$ that fit the estimated observations $F = (f_1, \dots, f_n)$, we can estimate the remaining cycles $X = (x_1, \dots, x_m)$ by the following equation:

$$X = A^{-1}(Y - C) \quad (3)$$

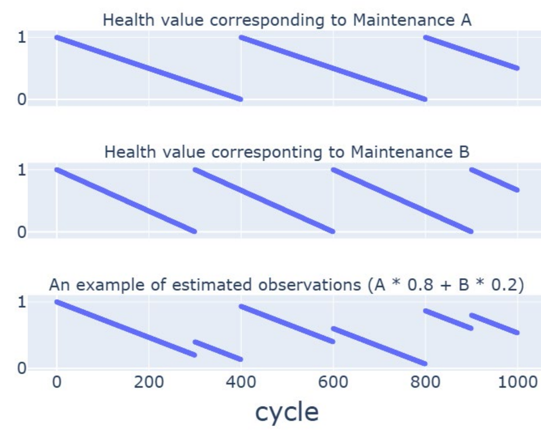

Figure 2. Maintenance Cycle Model.

4. ESTIMATION FOR HIGH PRESSURE TURBINE (HPT) AND HIGH PRESSURE COMPRESSOR (HPC) SHOP VISIT

We applied the maintenance cycle model to estimate remaining cycles for HPT and HPC shop visits.

The flow of the remaining cycle estimation for HPT and HPC is shown in Figure 3. Overview of the flow is described below:

(1) Feature Extraction: We selected the following features as described in Section 2:

y_e: isentropic efficiency

y_t: increment rate from T3 to T45, (T45-T3)/T3.

(2) Training: From the training data, we extracted features $Y = (y_e, y_t)$ as target variables, where Y_e is isentropic efficiency and Y_c is increment rate from T3 to T45. We

used remaining cycles data $X = (x_{HPT}, x_{HPC})$ as explanatory variables and trained a linear regression model for each ESN (Engine Serial Number).

(3) Model Fitting: As shown in Figure 4, the observation $Y = (y_e, y_t)$ contains significant fluctuation probably because they are influenced by various flight conditions. The fluctuation makes it difficult to precisely estimate the remaining cycles. To address this issue, we developed a model fitting method to extract clean observations to which the maintenance cycle models fit well. The method utilizes a zero-crossing method to find gaps by sudden changes in the trend of the observations. Then each trend is described by a line by fitting the model to the observation.

(4) Remaining Cycle Estimation: Once we obtain clean observation Y_{clean}, we can estimate X according to equation (3).

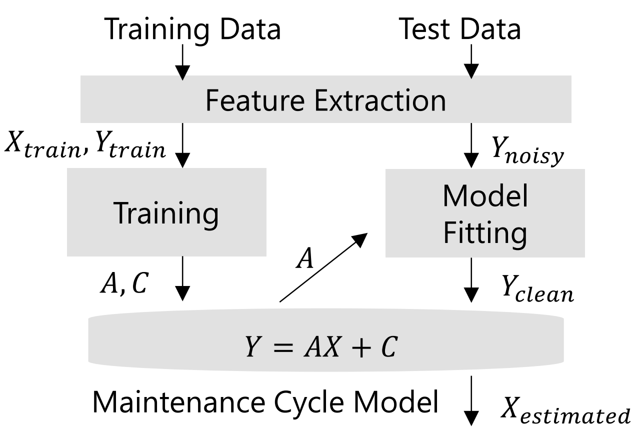

Figure 3. Flow of Remaining Cycle Estimation for HPT and HPC.

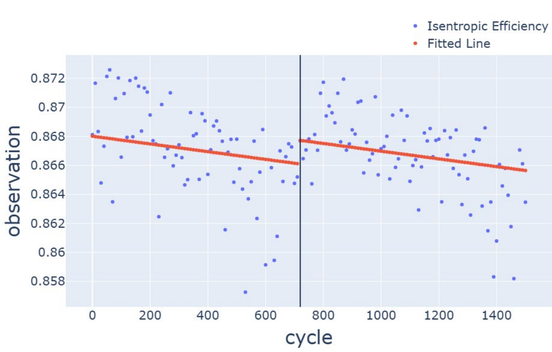

Figure 4. Model Fitting.

5. ESTIMATION FOR WATER-WASH (WW)

The remaining cycles of WW exhibit a low simple correlation with the features. Therefore, a different approach is needed compared to the maintenance cycle model. As a new approach, we utilized simulation data (NASA AGTF30 Simulation). Figure 5 shows the increment rate from T3 to T45 calculated from sensor values and simulations. From Figure 5, a significant similarity in the fluctuation patterns between the sensor values and simulations is observed. Therefore, we defined the difference between the sensor values and the simulation values as y_d, and the result after applying a moving average to y_d is shown in Figure 6. From Figure 6, it can be seen that spikes in y_d occur in cycles delineated by the red dashed line (Cycles_WW = 0).

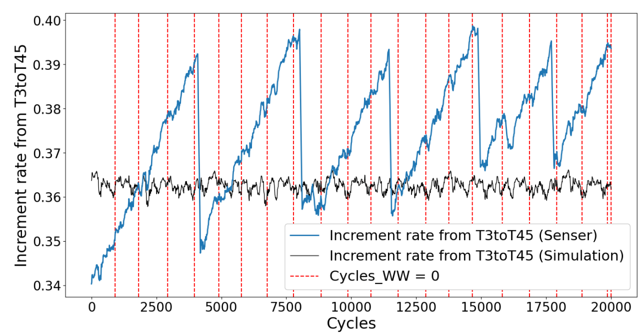

Figure 5. Increment Rate from T3 to T45 Calculated from Sensor Values and Simulations.

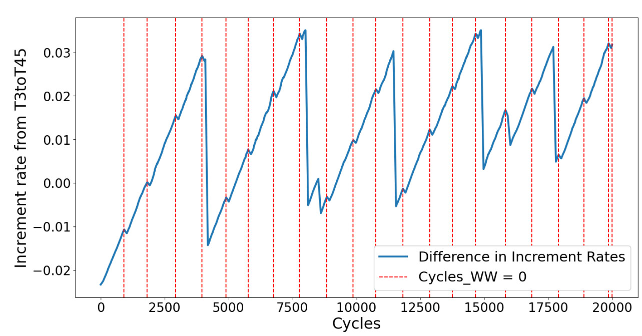

Figure 6. Difference in the Increment Rate from T3 to T45 Between Sensor Values and Simulations.

The outline of the remaining cycle estimation for WW is as follows:

(1) Feature extraction: We selected the following features:

y_d: Difference between y_t and y_{t_sim}, y_t-y_{t_sim}.

By applying a moving average to y_d, we reduced noise and clarified the trend.

y_{ma}: Moving average of y_d (window size = 10).

(2) Model: As shown in Figure 6, the spikes in y_{ma} occur over time, making time-series pattern recognition

essential. Furthermore, the changes in the spikes also include local features such as abrupt changes and noise, which need to be captured simultaneously. To address this problem, we utilized a CRNN model that excels in local feature extraction and learning long-term dependencies. The CRNN is a model that combines the local feature extraction capabilities of Convolutional Neural Networks (CNN) with the time-series dependency learning capabilities of Recurrent Neural Networks (RNN).

(3) Training: The CRNN was trained by dividing y_{ma} into sliding windows of width 128. ESN101 to ESN103 were used as the training data (5619 samples), while ESN104 was used as the unseen data (1873 samples).

(4) Remaining Cycle Estimation: By applying a moving average (window size = 3) to the Remaining Cycle regressed by the CRNN, we reduced noise.

6. ESTIMATION OPTIMIZATION

Taking the scoring rules into account, we aimed to optimize the estimation process. The optimizing process is as follows:

(1) Assumption of Probability Distribution: Suppose that initial estimation is 2500 cycles, we assume the probability distribution of the true value distributes around the initial estimation as shown in the first plot of Figure 7, where probability distribution function is Weibull distribution with a shape parameter of 4.0, and the characteristic life is set to align with the initial estimation.

(2) Minimization of the Expected Value of the Score: Assuming the probability distribution, we evaluate the expected value of the score for each estimated value of remaining cycles. By minimizing the expected value, we obtain the optimized estimation.

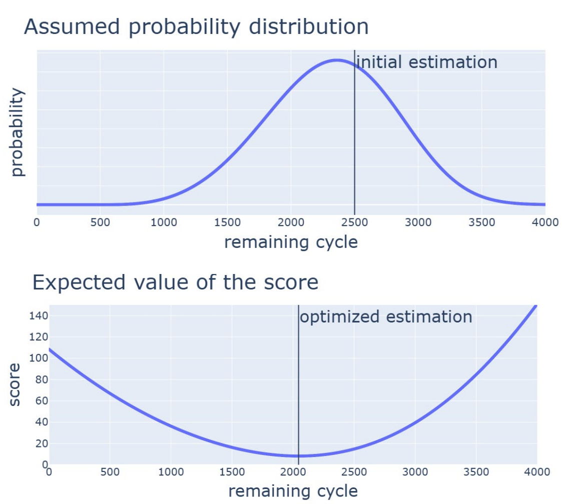

Figure 7. Estimation Optimization.

7. RESULTS AND DISCUSSION

Our method achieved a score of 48.56 on the validation data, placing it second among the competitors. This result suggests the effectiveness of our approach.

Table 2 shows the evaluation results using the training data. We randomly extracted 10 test datasets from each Engine Serial Number (ESN), and scores were calculated using cross-validation.

Table 2. Experimental Results.

	Initial estimation				Optimized estimation			
	WW	HPC	HPT	mean	WW	HPC	HPT	mean
score (mean)	29.35	92.35	20.38	47.36	20.93	35.27	16.45	24.22
score (max)	162.05	826.37	147.88	282.31	130.96	151.97	48.44	75.38

As shown in the table, the scores improved through estimation optimization. Notably, the maximum (worst) score value was 75.38, whereas the initial estimation was 282.31, indicating the stability of our method.

8. CONCLUSION

We presented a remaining cycle estimation method based on a maintenance cycle model. The model is simple yet fits the aircraft engine data in the PHM 2025 Data Challenge very well. The model-based method, along with the physics-informed feature exploration and the estimation optimization, yielded accurate and stable results.

REFERENCES

NASA AGTF30 Simulation. MATLAB Executable Steady-State Solver and Linearization Tool for the AGTF30 Engine Simulation (MEXLIN-AGTF30) , https://software.nasa.gov/software/LEW-20688-1